THE JOURNAL OF BIOLOGICAL CHEMISTRY
Vol. 279, No. 42, Issue of October 15, pp. 43595–43603, 2004
© 2004 by The American Society for Biochemistry and Molecular Biology, Inc.
Printed in U.S.A.

Amino Acid Residues Involved in Autophosphorylation and Phosphotransfer Activities Are Distinct in Nucleoside Diphosphate Kinase from *Mycobacterium tuberculosis**

Received for publication, February 16, 2004, and in revised form, July 28, 2004
Published, JBC Papers in Press, August 9, 2004, DOI 10.1074/jbc.M401704200

Sangeeta Tiwari‡, K. V. Radha Kishan, Tapan Chakrabarti, and Pradip K. Chakraborti§

From the Institute of Microbial Technology, Sector 39A, Chandigarh 160 036, India

Nucleoside diphosphate kinase (NdK) is a ubiquitous enzyme in both prokaryotes and eukaryotes and is primarily involved in the maintenance of cellular nucleotide pools. We have cloned *ndk* from *Mycobacterium tuberculosis* strain H37Ra and expressed it in *Escherichia coli* as a fusion protein with glutathione *S*-transferase. The purified protein, following thrombin cleavage and gel permeation chromatography, was found to be hexameric with a monomeric unit molecular mass of ~16.5 kDa. The protein exhibited nucleotide binding, divalent cation-dependent autophosphorylation, and phosphate transfer ability from nucleoside triphosphate to nucleoside diphosphate. Although UDP inhibited the catalytic activity of the recombinant protein, the classic inhibitors, like cromoglycate, 5′-adenosine 3′-phosphate, and adenosine 3′-phosphate 5′-phosphosulfate, had no effect on the activity. Among three histidine residues in the protein, His-117 was found to be essential for autophosphorylation. However, in subsequent phosphate transfer, we observed that His-53 had a significant contribution. Consistent with this observation, substitution of His-53 with either Ala or Gln affected the ability of the recombinant protein to complement NdK function in *Pseudomonas aeruginosa*. Furthermore, mutational analysis established critical roles for Tyr-50 and Arg-86 of the *M. tuberculosis* protein in maintaining phosphotransfer ability.

Nucleoside triphosphates or their deoxy derivatives (NTP/dNTP) are of fundamental importance for the survival of any living organism, because they act as precursors for synthesis of macromolecules like nucleic acids. Nucleoside diphosphate kinase (NdK)[1] plays a pivotal role in the maintenance of intracellular ratios of NTPs and dNTPs. This enzyme has very little specificity for the base or the sugar and catalyzes phosphotransfer reaction from a NTP/dNTP to a NDP through a ping-pong mechanism involving a high energy phosphorylated intermediate (1). NdK has been characterized from several prokaryotes and eukaryotes (2–6). Despite high homology in the amino acid sequence, the functional enzymes are tetrameric in several prokaryotes, whereas in eukaryotes they exist in hexameric form. The crystal structures of many NdKs with or without substrates have been determined, and they are highly conserved from *Escherichia coli* to human (43% identity) with polypeptides having a molecular size of ~15 to 18 kDa (7). Besides their role in maintaining NTP pools, NdKs have also been reported to participate in regulating a variety of cellular functions. Studies in bacteria have revealed that NdK is essential for cell growth and differentiation (2, 5). In *E. coli*, NdK has been shown to act as a protein kinase to phosphorylate histidine kinases like EnvZ and CheA, thereby suggesting its involvement in cross-talk with two component signal transduction systems (8). Its role in sequence-dependent DNA binding as well as transcription (9) and site-specific DNA cleavage (10, 11) has also been demonstrated. Interestingly, the DNase activity exhibited by both human and *E. coli* NdKs has been implicated in base excision repair (12). In *Drosophila melanogaster*, NdK was involved in development of wing disc cells (13). Several NdKs have been reported in humans. Although NdKA (NM23-H1) suppressed tumor metastasis in melanoma cells (14), NdKB (NM23-H2) has been shown to bind the promoter of c-*myc* oncogene to activate its transcription (15).

NdK has been found to be present in membranous, cytosolic, and secretory forms (16, 17). Interestingly, in *Pseudomonas aeruginosa*, interaction of NdK with different proteins has been shown to modulate the synthesis of GTP (17). Although the membrane-associated form of NdK in this bacteria could complex with the Ras-like protein Pra and/or pyruvate kinase, the cytosolic form interacted with elongation factor TU (Ref. 18 and references therein). Extracellular secretion of this enzyme has been reported in *Mycobacterium bovis* bacillus Calmette-Guérin (19), *P. aeruginosa* (20), *Trichenella spiralis* (21), and *Vibrio cholerae* (22). Because a large number of secretory proteins are usually produced by pathogens to adhere to or infect host cells, they have often been considered as target molecules for designing new vaccines as well as novel drug intervention strategies (23, 24). Therefore, being a secretory molecule in pathogens, NdK may be an important enzyme to study. In this context, we have focused on tuberculosis, a disease caused by *Mycobacterium tuberculosis* that is responsible for considerable human morbidity and mortality worldwide due to the rapid resurgence of drug resistant strains in recent years (25).

Analysis of the genome sequence of *M. tuberculosis* H37Rv (26) has revealed the presence of single *ndk* gene (Rv2445c). It has been reported that mycobacterial NdKs were secretory in nature and might be involved in virulence by the sequestration of ATP from macrophage surface-associated P2Z receptors (19).

* This work was supported in part by a research grant from the Department of Biotechnology, New Delhi, India, as part of a National Bioscience Award for Career Development to one of the authors (to P. K. C.). The costs of publication of this article were defrayed in part by the payment of page charges. This article must therefore be hereby marked "*advertisement*" in accordance with 18 U.S.C. Section 1734 solely to indicate this fact.

‡ Recipient of a Senior Research Fellowship from the Council of Scientific and Industrial Research, New Delhi, India.

§ To whom correspondence should be addressed. Tel.: 91-172-269-5215 (ext. 452); Fax: 91-172-269-0585; E-mail: pradip@imtech.res.in.

[1] The abbreviations used are: NdK, nucleoside diphosphate kinase; ABTS, 2,2′-azino-bis(3-ethylbenzthiazoline-6-sulfonic acid); FSBA, 5′-*p*-fluorosulfonylbenzoyl adenosine; GST, glutathione *S*-transferase; IPTG, isopropyl-β-D-thiogalactopyranoside; mNdK, *M. tuberculosis* nucleoside diphosphate kinase; PAP, 5′-adenosine 3′-phosphate; PAPS, adenosine 3′-phosphate 5′-phosphosulfate.

This is an Open Access article under the CC BY license.

Furthermore, it has also been reported to be cytotoxic in mouse macrophage cell lines (27). Although a 2.6-Å x-ray structure of NdK from *M. tuberculosis* (mNdK) has been solved (28), its detailed biochemical characterization is not available as yet. Therefore, we concentrated on the mNdK and studied the autophosphorylation as well as phosphotransfer activities of this recombinant protein through structure-function analysis. Our results argued that different amino acid residues are required for autophosphorylation and phosphotransfer activities in mNdK. Although the His-117 was essential for autophosphorylation of the protein, it was not involved in subsequent transfer of phosphate to NDPs. On the other hand, His-53, Tyr-50, and Arg-86 were critical for its phosphotransfer activity.

EXPERIMENTAL PROCEDURES

Materials—Restriction/modifying enzymes were obtained from New England Biolabs. All other fine chemicals, including ABTS, different nucleotides, proteinase K, thrombin, PAP, PAPS, FSBA, cromoglycate, and 4-aminoantipyrine were procured from Sigma Chemical Co. Oligonucleotides used in this study were custom synthesized (Biobasic Inc. or IDT). [γ-^{32}P]ATP and [α-^{32}P]dCTP were purchased from Jonaki Laboratories, the Board of Radiation and Isotope Technology, Hyderabad, India

PCR Amplification, Construction of Recombinant Plasmids, and Generation of Site-directed Mutants of mNdK—Genomic DNA was isolated from *M. tuberculosis* strain H37Ra as described previously (29) and used for PCR amplification of *ndk.* Primers (CT3: 5′-CATATGACCGAACGGACTCTGG 3′ and CT4: 5′-CTAGGCGCCGGGAAACCAG-3′) used for this purpose were designed based on the published *ndkA* (Rv2445c) sequence of *M. tuberculosis* (26). However, for expression of the protein in *E. coli or P. aeruginosa*, the start codon was changed to ATG instead of GTG and, accordingly, an NdeI site was incorporated in the primer CT3. The *ndk* gene (~411 bp) was PCR-amplified using the GC Rich PCR system (Roche Applied Science) following the manufacturer's recommended protocol. The gene was initially cloned in pT-Adv vector (pTAdv-NdK), and its nucleic acid sequence was determined using an automated sequencer (Applied Biosystems). This construct was subsequently used for subcloning the *M. tuberculosis ndk* gene in different vectors for its expression in heterologous hosts, like *E. coli* and *P. aeruginosa*. pTAdv-NdK was digested with NdeI and treated with DNA polymerase I (Klenow) to obtain a blunt-ended fragment. This fragment was subsequently digested with either HindIII or KpnI for subcloning into different vectors. Similarly, following XhoI digestion of pGEX-KG (30) or pSFFLAG-MAC (31), the fragments were treated with Klenow. The blunt-ended vectors were then digested with either HindIII (pGEX) or KpnI (pSFFLAG). Finally, the *M. tuberculosis ndk* gene was ligated to the appropriate vectors to yield pGEX-NdK or pSFFLAG-NdK and transformed in *E. coli* strain DH5α. Clones containing the gene of interest were confirmed by restriction analysis while junction sequencing was carried out to authenticate in-frame fusions.

Genomic DNA from *P. aeruginosa* type strain MTCC 1934 was extracted following procedures described elsewhere (32) and used for PCR amplification of a fragment of ~1.5 kb (nucleotide position 4,265,949–4,267,400 of the genome) containing 431 bp of *ndk* (nucleotide position 4,266,469–4,266,900; coding sequence at −1 frame). Primers, CT34 (5′-CAACTAGTCTAGACGACATTGGTGATGGCG-3′; XbaI site incorporated) and CT35 (5′-CAAAACGAGCTCCCATCAACCAGGTGTC-3′; SacI site introduced) used for this purpose were designed from the published *P. aeruginosa* genome sequence (33). The PCR-amplified fragment was cloned in pUC19 (pPN1). Subsequently, a kanamycin cassette of ~1.3 kb (34) was introduced at the unique NruI site of pPN1 to obtain pPNK1. Thus this plasmid had the kanamycin cassette inserted in the *ndk* open reading frame and was used for gene disruption in *P. aeruginosa*.

Site-directed mutants of *M. tuberculosis ndk* (K10A, K29A, H49A, H49Q, Y50F, H53A, H53Q, R86A, R104A, H117A, H117Q, and S119A) were generated using pGEX-NdK as template following the overlap extension PCR method (35, 36). CT31 (in addition to nucleotides in CT3, an XhoI site was incorporated at the 5′-end) and CT32 (HindIII site was added in CT4) were used as external primers. The different internal primers used in generating mutants will be provided upon request. Different mutants (H49A, H49Q, H53A, H53Q, H117A, H117Q, and Y50F) were initially digested with HindIII, treated with Klenow, and finally excised by XhoI digestion. These constructs were then cloned into the XhoI/SmaI sites of pSFFLAG-MAC and used to assess the ability of different mutants to complement NdK function in *P. aeruginosa* (please see below).

Expression and Purification of Recombinant Protein—The pGEX-NdK or different mutants were transformed into *E. coli* strain BL21(DE3) for overexpression and subsequent purification of proteins. Overnight cultures of these clones (~15 h at 37 °C in LB broth containing 100 μg/ml ampicillin) were re-inoculated and grown to an A_{600} of ~0.6. Cells were then induced with 0.2 mM IPTG, harvested after 3 h, and suspended in lysis buffer (50 mM Tris, pH 8, containing 5 mM EDTA, 50 mM NaCl, 1 mM phenylmethylsulfonyl fluoride, 1 μg/ml of pepstatin, and 1 μg/ml leupeptin). Following lysozyme treatment (30 min at 4 °C), cells were sonicated and the supernatant fraction was collected after centrifugation (17,600 × *g* for 15 min at 4 °C). This fraction was loaded onto a glutathione-agarose affinity column and cleaved with thrombin (55.5 units/5 ml of bed volume) following the manufacturer's recommended protocol. The protein (mNdK or different mutants following removal of GST tag) obtained in this way was subjected to gel permeation chromatography on a fast-protein liquid chromatography unit using a Superdex 200 column. Finally, the purified protein was eluted with elution buffer (50 mM Tris, pH 8, containing 1 mM EDTA), and its concentration was estimated following Bradford's method (37).

Gene Disruption and Complementation—The *ndk* gene of *P. aeruginosa* type strain was disrupted using the pPNK1 gene disruption cassette following the method described elsewhere (38). Twenty-five transformants were selected in LB plates supplemented with kanamycin (200 μg/ml). They were further confirmed by Southern analysis using [α-^{32}P]dCTP-labeled probes (kanamycin-resistant gene and DNA fragment containing *P. aeruginosa ndk*) following the standard protocol (39). As expected, SacI digestion of genomic DNA from *ndk*-disrupted transformants yielded a fragment of ~10.8 kb compared with that of ~9.5 kb in wild type cells. One of these transformants was randomly chosen to carry out experiments and was designated as WT^{d}. For complementation studies, *ndk* (both *M. tuberculosis* and *P. aeruginosa*) or other mutants were transformed in WT^{d}, and the expression was confirmed by Western blotting.

Autophosphorylation and Phosphotransfer Assays—Autophosphorylating abilities of mNdK or different mutants were assessed by incubating purified proteins in 1× kinase buffer (50 mM Tris-Cl, pH 7.5, 50 mM NaCl, 300 μM $MgCl_2$) in the presence of 2 μCi of [γ-^{32}P]ATP at 24 °C for 1 min. SDS sample buffer (30 mM Tris-Cl, pH 6.8, 5% glycerol, 2.5% β-mercaptoethanol, 1% SDS, and 0.01% bromphenol blue) was added to terminate the reaction. Samples were boiled for 5 min and resolved on 12% SDS-PAGE gels. Gels were analyzed in a phosphorimaging device (Bio-Rad) using Quantity One software and exposed to Kodak X-Omat/AR film for autoradiography (29). To monitor the effect of different divalent cations on the autophosphorylating abilities of mNdK, they (Ca^{+2}/Co^{+2}/Cu^{+2}/Mn^{+2}/Zn^{+2}) were added in the kinase buffer instead of $MgCl_2$.

Phosphotransfer activities of mNdK or different mutants were monitored in a colorimetric assay performed in microtiter plates (40). Briefly, in a 50-μl reaction volume mNdK protein (1–10 ng) was mixed with several ingredients (50 mM Tris-HCl, pH 7.4, 5 mM $MgCl_2$, 75 mM KCl, 1.5 mM 4-aminoantipyrene, 1 mM glycerol, 1.5 mM 3,5-dichlorophenolsulfonic acid, 0.5 mg/ml bovine serum albumin, 1 unit/ml glycerokinase, 2.5 units/ml glycerol-3-phosphate oxidase, 2.5 units/ml peroxidase) along with dGTP (1 mM) as the phosphate donor nucleotide and ADP (5–250 μM) as the substrate. This was followed by incubation (0–8 min) at 24 °C and subsequent monitoring of enzyme activity at 490 nm in an enzyme-linked immunosorbent assay plate reader. The values obtained were corrected by subtracting the blank readings (no significant difference was noticed when assays were carried out with all ingredients except either substrate or mNdK or dGTP). Standard curves were prepared with known amounts (5–200 μM) of ATP (omitting dGTP, ADP, and mNdK in reaction mixtures), and the kinase activity of mNdK was expressed as micromoles of ATP produced/min/mg of protein. A preincubation step (20 min or 3 h at 24 °C) with the protein was included in the assays to monitor the influence of varied concentrations of inhibitors (AMP, cyclic AMP, cromoglycate, PAP, PAPS, and UDP).

Western Blotting—Polyclonal antibody against mNdK was raised in rabbit following the method described earlier (36) and used for monitoring the expression of mNdK or mutant proteins by Western blotting. The antisera also showed cross-reactivity to NdK of *P. aeruginosa.* Samples (100 ng to 10 μg of protein/slot) were resolved on SDS-PAGE gels and transferred to nitrocellulose membranes. Blots were probed with primary (anti-mNdK or anti-GST) and secondary (horseradish peroxidase-conjugated anti-rabbit or anti-mouse IgG) antibodies and processed with the ECL detection system (Amersham Biosciences). The

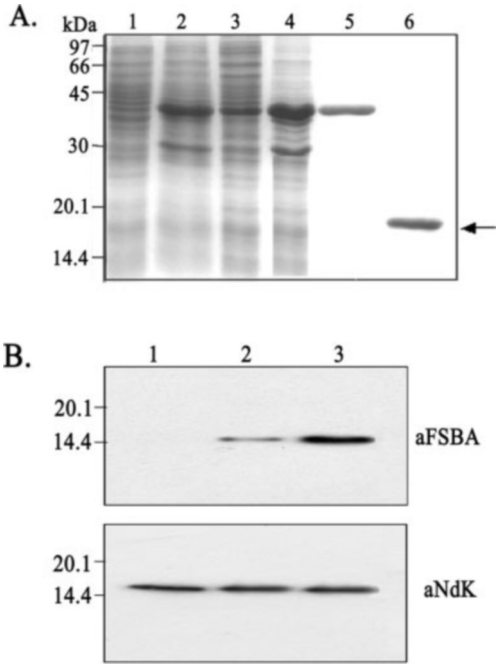

FIG. 1. **Purification of mNdK expressed in *E. coli* (*A*) and detection of its ATP-binding ability (*B*).** Overnight cultures of BL21(DE3) cells transformed with pGEX-NdK were processed for purification as described under "Experimental Procedures." *A*, protein samples at various stages of purification were subjected to 12% SDS-PAGE followed by Coomassie Brilliant Blue staining. *Lane 1*, crude extract of cells harboring plasmid pGEX-NdK without IPTG induction; *lane 2*, crude extract of cells harboring plasmid pGEX-NdK induced with IPTG; *lane 3*, low speed supernatant fraction; *lane 4*, pellet fraction obtained after low speed centrifugation; *lane 5*, glutathione-agarose resin purified fusion protein; and *lane 6*, purified mNdK obtained after thrombin cleavage followed by gel permeation chromatography. The *arrow* indicates position of purified mNdK containing 16 amino acids (PGISGGGGGILDSMGR) from GST tag. Numbers denote the position of molecular weight standards. *B*, purified mNdK following incubation with FSBA was subjected to SDS-PAGE and immunoblotting using anti-FSBA (*aFSBA*) or anti-mNdK (*aNdK*) antibodies. *Lane 1*, mNdK with no FSBA; *lane 2*, mNdK with 1 mM FSBA; *lane 3*, mNdK with 3 mM FSBA.

ATP-binding ability of the recombinant mNdK was monitored by labeling the protein with a nonhydrolyzable ATP analogue, FSBA, followed by detection through Western blotting using anti-FSBA antibody (Roche Applied Science).

Structural Analysis—Analysis of all available NdK structures, including that of mNdK (Protein DataBank accession number 1K44 and Ref. 28), were done using either 'O' program (41) or ICM (www.molsoft.com) on an SGI O2 graphics system.

RESULTS

Overexpression of mNdK—The *ndk* gene from *M. tuberculosis* strain H37Ra was amplified by PCR and cloned in the pT-Adv vector. Sequencing of this fragment indicated 100% identity at the nucleotide level with the published *ndkA* sequence of the pathogenic strain, H37Rv, of *M. tuberculosis*. To monitor expression of mNdK as a fusion protein with GST, pGEX-NdK was transformed into *E. coli* strain DH5α or BL21(DE3). Several colonies harboring the expression plasmid were obtained in both hosts. On SDS-PAGE gels, however, cell lysates prepared from *E. coli* strain DH5α exhibited two IPTG-induced bands (~41 and ~43 kDa). On the other hand, the expected ~43 kDa fusion protein was observed in cell lysates of *E. coli* strain BL21(DE3) and therefore was used in subsequent studies (Fig. 1*A*). Approximately 20% of the expressed protein was found to be in the soluble fraction (Fig. 1*A*, *lane 3*). The fusion protein was purified by glutathione-agarose affinity chromatography (Fig. 1*A*, *lane 5*) and checked by Western blotting using anti-GST antibody (data not shown). GST-mNdK protein was treated with thrombin, further purified through a glutathione-agarose affinity column, and subjected to gel permeation chromatography. The purified mNdK protein containing 16 amino acids from the GST tag was eluted as a single peak in a Superdex 200 column and exhibited a molecular mass of 107 ± 2.56 kDa (mean ± S.D., $n = 9$). The same sample revealed a molecular mass of 16.5 ± 0.45 kDa (mean ± S.D., $n = 12$) on SDS-PAGE (Fig. 1*A*, *lane 6*). Western blotting with anti-mNdK antibody also recognized the purified protein (Fig. 1*B*). Considering the presence of 16 amino acids from GST tag in the mNdK, the molecular weight determined by SDS-PAGE analysis was found to be the same as has been predicted from the sequence. Thus our data support a possible hexameric conformation of the active form of mNdK, which is consistent with the value obtained following crystal structure analysis of the protein from *M. tuberculosis* pathogenic strain H37Rv (28).

mNdK Is a Nucleotide-binding Protein—The nucleotide binding ability of different NdKs has already been established (1, 42). To gain insight on this aspect, we utilized a nonhydrolyzable ATP analogue, FSBA, which binds to the nucleotide-binding site of proteins through covalent attachment (43). Following the labeling of protein (purified in borate buffer) with FSBA (1 or 3 mM) or treating with Me_2SO (solvent control), samples were subjected to SDS-PAGE and immunoblotting using anti-FSBA antibody. As shown in Fig. 1*B*, anti-FSBA antibody recognized only those samples that were incubated with FSBA (*lanes 2* and *3*). On the other hand, anti-mNdK antibody recognized all samples of this blot after being stripped (Fig. 1*B*). Although nonspecific binding of FSBA to mNdK could not be ruled out in our experimental set-up, the evidence we presented strongly suggested that this recombinant protein does bind nucleotides. Therefore, our results corroborated a recent study where the nucleotide binding ability of NdK from *M. tuberculosis* strain H37Rv was established using a different approach (27).

mNdK Exhibits Autophosphorylation and Phosphotransfer Ability—The autophosphorylating ability of mNdK was monitored by incubating it with [γ-^{32}P]ATP in the presence of Mg^{+2} followed by separation of the reaction products by SDS-PAGE and identification of the labeled proteins in a phosphorimaging device as well as by autoradiography of the dried gels. *In vitro* assays revealed that mNdK was capable of phosphorylating itself in a concentration-dependent manner (Fig. 2*A*, *lanes 2–7*), whereas heat-inactivated (100 °C for 5 min) protein did not show any activity (Fig. 2*A*, *lane 1*). The protein was able to autophosphorylate over a broad pH range of 3–12 (data not shown). As shown in Fig. 2*B*, divalent cations were essential for the autophosphorylation of mNdK (compare *lane 1* with *lanes 2–7*). Interestingly, autophosphorylation of this protein was detectable in the presence of all divalent cations (Ca^{+2}, Co^{+2}, Cu^{+2}, Mg^{+2}, Mn^{+2}, and Zn^{+2}) tested (Fig. 2*B*). Among the different inhibitors tested (AMP, cyclic AMP, and UDP), only UDP affected the autophosphorylation of mNdK. Surprisingly, cromoglycate, which is a known inhibitor of histidine phosphorylation (44), had no significant effect (Fig. 2*C*, *lanes 8* and *9*).

We further investigated the phosphotransfer activity of mNdK employing an enzyme-coupled assay using dGTP and ADP as donor and acceptor nucleotides, respectively. To determine the kinetic parameters, purified enzyme was incubated (up to 8 min at 24 °C) with increasing concentrations of ADP, and the activity was measured at every minute (Fig. 3, *inset A* shows a representative plot). The rate of reaction (amount of ATP generated/min) was calculated from the standard curve (see "Experimental Procedures") and plotted as a function of substrate concentration. This yielded a typical Michaelis-Menten curve (Fig. 3). The K_m

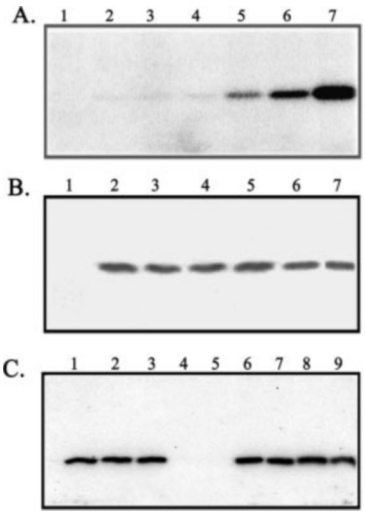

FIG. 2. **Autophosphorylation of mNdK.** Autophosphorylation of the mNdK was monitored by incubating purified protein with [γ-^{32}P]ATP followed by separation of the reaction products by SDS-PAGE. The labeled proteins were localized in a phosphorimaging device or by autoradiography of the dried gel (see "Experimental Procedures"). *A*, autophosphorylation with 12.5 (*lane 2*), 25 (*lane 3*), 50 (*lane 4*), 100 (*lane 5*), 250 (*lane 6*), and 500 (*lane 7*) ng of purified mNdK along with 500 ng of heat-inactivated protein (*lane 1*) in the presence of 300 μM of Mg^{+2}. *B*, the effect of divalent cations. Autophosphorylation of mNdK (250 ng of protein/reaction) was carried out in the absence (*lane 1*) or presence of 300 μM of Mg^{+2} (*lane 2*), Mn^{+2} (*lane 3*), Ca^{+2} (*lane 4*), Zn^{+2} (*lane 5*), Co^{+2} (*lane 6*), and Cu^{+2} (*lane 7*). *C*, the effect of different inhibitors. *Lane 1*, no inhibitor; *lane 2*, 2.5 mM AMP; *lane 3*, 5 mM AMP; *lane 4*, 2.5 mM UDP; *lane 5*, 5 mM UDP; *lane 6*, 20 mM cyclic AMP; *lane 7*, 40 mM cyclic AMP; *lane 8*, 50 mM cromoglycate; and *lane 9*, 100 mM cromoglycate.

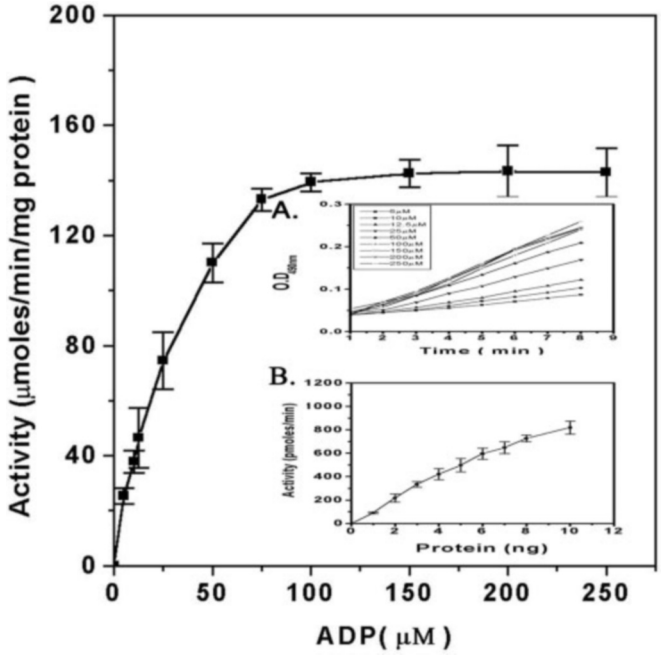

FIG. 3. **Phosphotransfer activity of mNdK.** Kinetics of ATP formation by purified mNdK (5 ng of protein/reaction) was determined using dGTP and ADP as donor and acceptor nucleotides, respectively. Purified enzyme was incubated with increasing concentrations of substrate (ADP) for 8 min (*inset*: *A*, shows a representative experiment). The amount of ATP generated per minute was then calculated from a standard curve as described under "Experimental Procedures" and plotted as a function of substrate concentrations. The enzyme activity with increasing amounts of protein (0–10 ng) was also monitored using 50 μM ADP (*inset*: *B*). The reproducibility was checked in six independent experiments.

TABLE I
Effect of inhibitors on phosphotransfer activity of mNdK

mNdK was preincubated with different inhibitors, and phosphotransfer activity was assessed as described under "Experimental Procedures." AMP, cyclic AMP, UDP, and cromoglycate were used in the range of 1–100 mM, whereas PAP and PAPS were used in the range of 1 μM to 1 mM. IC_{50} values were calculated, and results are expressed as mean ± S.D.

Inhibitor	IC_{50}	Number of experiments
	mM	
AMP	1.90 ± 0.26	3
Cyclic AMP	26.70 ± 2.88	3
UDP	1.57 ± 0.06	3
PAP	ND[a]	4
PAPS	ND	3
Cromoglycate	90.00 ± 13.22	3

[a] ND, not detectable.

and V_{max} values obtained from a Lineweaver-Burk plot were ~24 μM and ~171 μmol/min/mg of protein, respectively (see Table II). Furthermore, there was a linear increase (r = 0.989) in the enzyme activity with increasing concentrations of protein (Fig. 3, *inset B*). AMP, cyclic AMP, and UDP inhibited the enzyme activity considerably (Table I). As reflected in the IC_{50} (the concentration of inhibitor resulting in 50% inhibition) values, AMP and UDP were potent inhibitors compared with cyclic AMP. However, unlike other NdKs (44, 45), the phosphotransfer activity of mNdK (Table I) was not affected by either cromoglycate or 3′-phosphate nucleotides (PAP or PAPS). Thus our results highlighted the distinction in the behavior of mNdK compared with other bacterial homologues.

Role of Histidine Residues in Functionality of mNdK—Primary sequence analysis of mNdK revealed the presence of three histidine residues at amino acid positions 49, 53, and 117. Because mNdK is a histidine kinase, we examined the role of histidine residues in autophosphorylation as well as in phosphotransfer activities. Six different mutants were generated for this purpose by replacing each histidine with either alanine or glutamine (H49A, H49Q, H53A, H53Q, H117A, and H117Q). Expression of all the mutants was authenticated by the Western blot analysis using anti-mNdK antibody (Fig. 4*A*). As shown in Fig. 4*B*, the autophosphorylating ability was unaffected in each of the H49A, H49Q, H53A, and H53Q mutants. On the other hand, mutations at His-117 (H117A or H117Q) completely abolished the autophosphorylating ability. We therefore examined the effect of these mutations on the phosphotransfer activities of mNdK. Like autophosphorylation, the H49A or H49Q mutant proteins exhibited phosphotransfer activity at par with the wild type enzyme as reflected in the K_m, V_{max}, and k_{cat}/K_m values (Table II). Surprisingly, although H53A and H53Q showed K_m values similar to that of the wild type protein, the turnover rates were significantly reduced in these mutants (Table II). Thus our results argued for a role of the His-53 residue in the phosphotransfer activity of mNdK. As expected, neither of the H117A and H117Q mutants exhibited any detectable phosphotransfer activity. This appears to be contradictory to the results obtained with NdK from *M. tuberculosis* pathogenic strain H37Rv despite its absolute sequence identity at the nucleotide level with the nonpathogenic H37Ra strain (27). To resolve such a discrepancy, we therefore investigated the effect of these mutations on mNdK function.

It has been shown that in *ndk*-inactivated mutants of *P. aeruginosa*, pyruvate kinase maintains NTP pools. Interestingly, this mutant exhibited slow growth in the presence of Tween 20, a pyruvate kinase inhibitor (5). We therefore constructed a *ndk*-disrupted strain of *P. aeruginosa* (WT^d) by inactivating the gene via homologous recombination with pPNK1 (see "Experimental Procedures"). Crude lysates prepared from

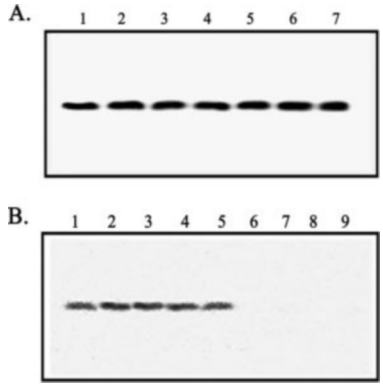

FIG. 4. **Role of histidine residues on autophosphorylating ability of mNdK.** Mutants of mNdK (H49A, H49Q, H53A, H53Q, H117A, and H117Q) were generated. They were expressed and purified as outlined under "Experimental Procedures." *A*, Western blot analysis of the mutant proteins using anti-mNdK antibody. *Lane 1*, wild type; *lane 2*, H49A; *lane 3*, H49Q; *lane 4*, H53A; *lane 5*, H53Q; *lane 6*, H117A; and *lane 7*, H117Q. *B*, autophosphorylating ability of various mutants was assessed using different amounts of protein (250 ng for wild type, H49A/H49Q, and H53A/H53Q and 250 ng or 2.5 μg for H117A/H117Q) in the assay. *Lane 1*, wild type; *lane 2*, H49A; *lane 3*, H49Q; *lane 4*, H53A; *lane 5*, H53Q; *lane 6*, 250 ng of H117A; *lane 7*, 2.5 μg of H117A; *lane 8*, 250 ng of H117Q; *lane 9*, 2.5 μg of H117Q.

TABLE II
Kinetics of kinase activity exhibited by mNdK mutants

Phosphotransfer assays were carried out as described under "Experimental Procedures" following the incubation of purified protein (5 ng/reaction) with different concentrations (5–250 μM) of ADP. K_m and V_{max} values were calculated from Lineweaver-Burk plots, and the results are expressed as mean ± S.D. For calculating k_{cat} values, the molecular mass of recombinant mNdK was considered as 16.5 kDa. The reproducibility was checked in at least three independent experiments carried out in a set.

	K_m	V_{max}	k_{cat}/K_m
	μM	μmol/min/mg	$\mu M^{-1}\ min^{-1}$
WT	23.70 ± 1.40	170.86 ± 30.00	12.14 ± 2.60
H49A	23.56 ± 1.05	198.93 ± 2.57	13.93 ± 0.61
H49Q	23.50 ± 1.93	154.10 ± 24.01	10.78 ± 0.90
H53A	23.21 ± 0.35	36.59 ± 1.05	2.59 ± 0.09
H53Q	23.62 ± 3.56	96.32 ± 11.90	6.75 ± 0.23
H117A	ND[a]	ND	ND
H117Q	ND	ND	ND

[a] ND, not detectable.

WT^d cells did not show any NdK-specific bands after Western blotting with anti-mNdK antibody (see below Fig. 5*C*, *lane 2*). This observation, therefore, emphasized that gene disruption affected the expression of NdK in WT^d at the protein level. As expected, WT^d showed slow growth compared with wild type cells in LB medium supplemented with 0.1% Tween 20 (Fig. 5*A*, *left panel*). However, WT^d harboring pSFFLAG-NdK exhibited a growth curve quite comparable to that of the wild type *P. aeruginosa* in the presence of Tween 20 (Fig. 5*A*, *right panel*). We further studied the ability of different histidine mutants of mNdK to compliment the growth defect of WT^d in the presence of Tween 20. Both H49A and H49Q behaved like the wild type mNdK (Fig. 5*B*, *left panel*). H117A or H117Q, however, showed a growth pattern identical to that of the WT^d, thereby suggesting an inability of these mutants to complement NdK function (Fig. 5*B*, *right panel*). Surprisingly, as shown in Fig. 5*B* (*middle panel*), the H53Q and H53A mutants showed either partial or no complementation of NdK function in WT^d. As evidenced by Western analysis, this discrepancy did not arise out of any differences in expression of these mutants at the protein level (Fig. 5*C*). Thus we concluded that, in addition to His-117, His-53 is a critical residue in the mNdK protein for phosphotransfer activity as well as in complementing its function in WT^d.

Contributions of the Active Site Residues in mNdK Activity—A detailed visual comparison of the structures of mNdK and its human counterpart, Nm23-H1, was made using molecular modeling software. This analysis revealed that the residues involved in nucleotide binding and enzyme activities are essentially unchanged between the two enzymes. Therefore, several point mutants (K10A, K29A, Y50F, R86A, R104A, and S119A) were generated (please see Fig. 6*A*) to evaluate the role of various conserved residues on the autophosphorylation as well as phosphotransfer activities of mNdK. One of these residues (Lys-29) would appear to be important for maintaining the hexameric conformation of the protein as a dimer of two trimers. Therefore, mutation of this lysine residue to alanine was expected to affect both its quaternary structure and activity, because the subunit interface(s) of the protein overlaps with its active site. As anticipated, the K29A mutant showed no autophosphorylation or phosphotransfer activities (Fig. 6, *B* and *C*). We had envisaged that two positively charged residues at the active site (Arg-86 and -104) could play a structural role in maintaining the geometry of the active site while also being involved in interactions with the α- and β-phosphates of NDP. Thus, mutations in these residues would be likely to affect both the autophosphorylation as well as phosphotransfer activities of mNdK. Although both mutants (R86A and R104A) lacked phosphotransfer activities, they exhibited remarkable differences in autophosphorylating abilities (Fig. 6*C*). Although the R104A did not show any autophosphorylating ability, the R86A retained it. This observation, therefore, indicated a differential role of Arg-86 residue of mNdK in autophosphorylation and phosphotransfer. Mutants K10A and Y50F showed no phosphotransfer activity (Fig. 6*C*), presumably due to destabilization of the network of hydrogen bonds made by the amino group of lysine and the phenyl hydroxyl of tyrosine (46). The relative autophosphorylating abilities of K10A and Y50F mutants, as determined by scanning the band intensities with 250 ng of protein in a phosphorimaging device, were ~10 and ~20%, respectively, of that obtained with the wild type enzyme (Fig. 6*B*). Surprisingly, a 10-fold excess of Y50F mutant protein in these assays restored the autophosphorylation activity to a level comparable to the wild type (*inset*, Fig. 6*B*). This observation was further confirmed by varying either protein concentration or reaction time in autophosphorylation assays with Y50F mutant (data not shown). The phosphotransfer activity of the Y50F mutant, on the other hand, could not be detected even when using a 50-fold excess of Y50F protein (*inset*, Fig. 6*C*). The identical mutation at the homologous tyrosine residue of *Dictyostelium discoideum* NdK retained negligible (~2% of wild type) phosphotransfer activity (47). Furthermore, the Y50F mutant was unable to complement NdK function in *P. aeruginosa*, thus suggesting the importance of this tyrosine residue in mNdK activity (data not shown). The S119A mutant was not affected in either autophosphorylation or phosphotransfer activities (Fig. 6, *B* and *C*). Structural analysis suggested that the only role of this serine residue is to stabilize the charge of His-117 upon phosphorylation. Therefore, the absence of any effect of this mutation on activity is not surprising. The migration of the wild type mNdK on SDS-PAGE gels was indistinguishable from that of the various mutants (Fig. 6*D*). However, in conformity of the expectation that certain mutants would affect the quaternary structure of the protein, R104A, K10A, and K29A exhibited differences in migration on native PAGE gels (Fig. 6*E*, *lanes 4*, *5*, and *7*). Thus, in summary, our results confirm the significant contributions of residues like Arg-86 and Tyr-50 in maintaining the phosphotransfer activity of mNdK.

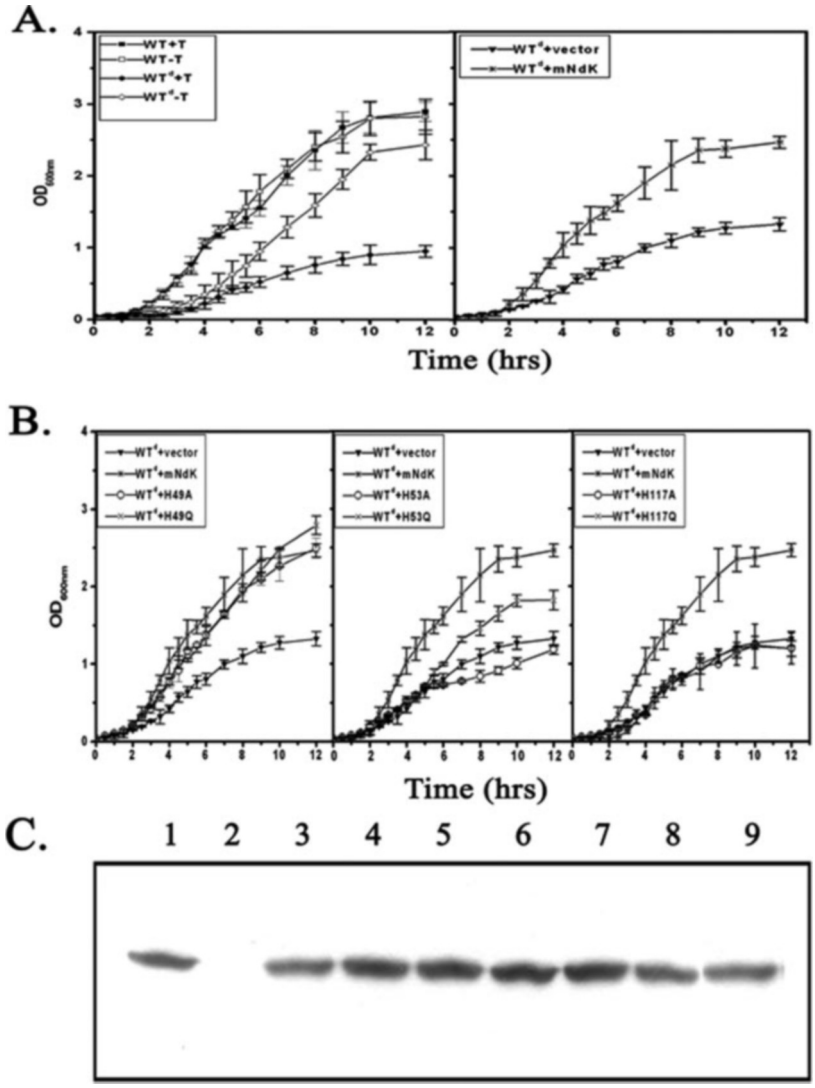

FIG. 5. **Functional complementation of mNdK mutants in *P. aeruginosa*.** WT^d, the *ndk*-disrupted strain of *P. aeruginosa*, was constructed as described in the text. Wild type or different mutants (H49A/H49Q, H53A/H53Q, and H117A/H117Q) of *M. tuberculosis ndk* were cloned into pSFFLAG-MAC. Following transformation in WT^d, complementation of NdK function by recombinant proteins, wild type (*A*), or mutants (*B*) was assessed by monitoring the growth pattern (OD_{600}) in LB medium supplemented with or without 0.1% Tween 20 for 12 h. In *A*: *left panel*, growth profiles of *P. aeruginosa* strain MTCC 1934 (*WT*) and WT^d were monitored in the presence (+) or absence (−) of 0.1% Tween 20 (*T*). *Right panel*, the growth of WT^d harboring *M. tuberculosis ndk* or pSFFLAG-MAC (vector) in the presence of 0.1% Tween 20. *B*, growth profile of WT^d harboring H49A/H49Q (*left panel*) or H53A/H53Q (*middle panel*) or H117A/H117Q (*right panel*) in the presence of 0.1% Tween 20. *C*, expression of NdK in *P. aeruginosa* strain MTCC 1934 and WT^d harboring either vector or *M. tuberculosis ndk* or different mutants of mNdK. Lysates of the cells were prepared, and Western blotting using anti-mNdK antibody was carried out to monitor the expression of wild type and mutant proteins. *Lane 1*, *P. aeruginosa* and *lanes 2–9*, WT^d transformed with either pSFFLAG-MAC (*lane 2*), mNdK (*lane 3*), H49A (*lane 4*), H49Q (*lane 5*), H53A (*lane 6*), H53Q (*lane 7*), H117A (*lane 8*), or H117Q (*lane 9*).

DISCUSSION

NdK is a ubiquitous enzyme, which is in keeping with its role of maintaining cellular NTP pools and has been reported to be involved in several regulatory processes in both prokaryotes and eukaryotes (1, 13–15). Recent studies further indicated that this enzyme, which has largely been shown to be cytoplasmic, could be secreted in pathogenic bacteria like *M. tuberculosis*, *P. aeruginosa*, and *V. cholerae* (20, 22, 27). Although the physiological relevance for the secretory nature of NdK is not clear, the importance of this enzyme in host-pathogen interaction has already been postulated (19). This has led to renewed interest in bacterial NdKs in recent years. In this context, we have focused on NdK from *M. tuberculosis*. Despite the availability of the recombinant NdK protein and its 2.6-Å x-ray structure, a detailed biochemical characterization of this enzyme has not yet been conducted. In this study we therefore carried out structure-function analyses of mNdK, with particular attention to its autophosphorylation and phosphotransfer activities.

The mNdK was expressed as a fusion protein with GST utilizing an *E. coli*-based expression system (Fig. 1*A*). After thrombin cleavage, the purified protein retained 16 amino acids from the GST tag at the amino-terminal end. This ~16.5-kDa (calculated molecular mass 16.04 kDa) recombinant NdK protein was used in our studies. Sequence analysis of NdKs from different sources, including *M. tuberculosis*, do not exhibit typical nucleotide binding motifs (G*XX*GK or D*XX*G) even though they bind NTP/dNTP (1, 27). As expected, we also observed nucleotide binding with this recombinant protein, as evidenced by the results with FSBA (Fig. 1*B*). Because NdKs have been shown to transfer the terminal phosphate of N_1TP to N_2DP to form N_2TP via an autophosphorylated intermediate, we utilized [γ-^{32}P]ATP for monitoring the autophosphorylation of this recombinant protein. The phosphotransfer activity of mNdK, on the other hand, was assessed using dGTP and ADP as phosphate donor and acceptor, respectively. As has been observed with other bacterial NdKs (1), the recombinant protein exhibited both autophosphorylation (Fig. 2) and phosphotransfer (Fig. 3) activities. However, the enzymatic activity of mNdK was found to be resistant to known inhibitors such as cromoglycate, PAP, and PAPS (Fig. 2 and Table I). Furthermore, unlike *E. coli* NdK (8), mNdK protein was unable to participate in signal transduction processes as a protein phosphotransferase (data not shown). Thus, although the *M. tuberculosis* protein shares many of the characteristics of various bacterial NdKs, subtle differences do exist in its behavior, which makes mNdK distinct from the others.

Analysis of the crystal structure revealed that mNdK is a hexamer with D3 symmetry despite a sequence divergence in the Kpn loop and a shorter carboxyl terminus (28). Because the NdK proteins from different sources exhibit high homology (and >40% amino acid sequence identity) at the active site, residues at this region were expected to be highly conserved and structurally quite similar to the eukaryotic homologues

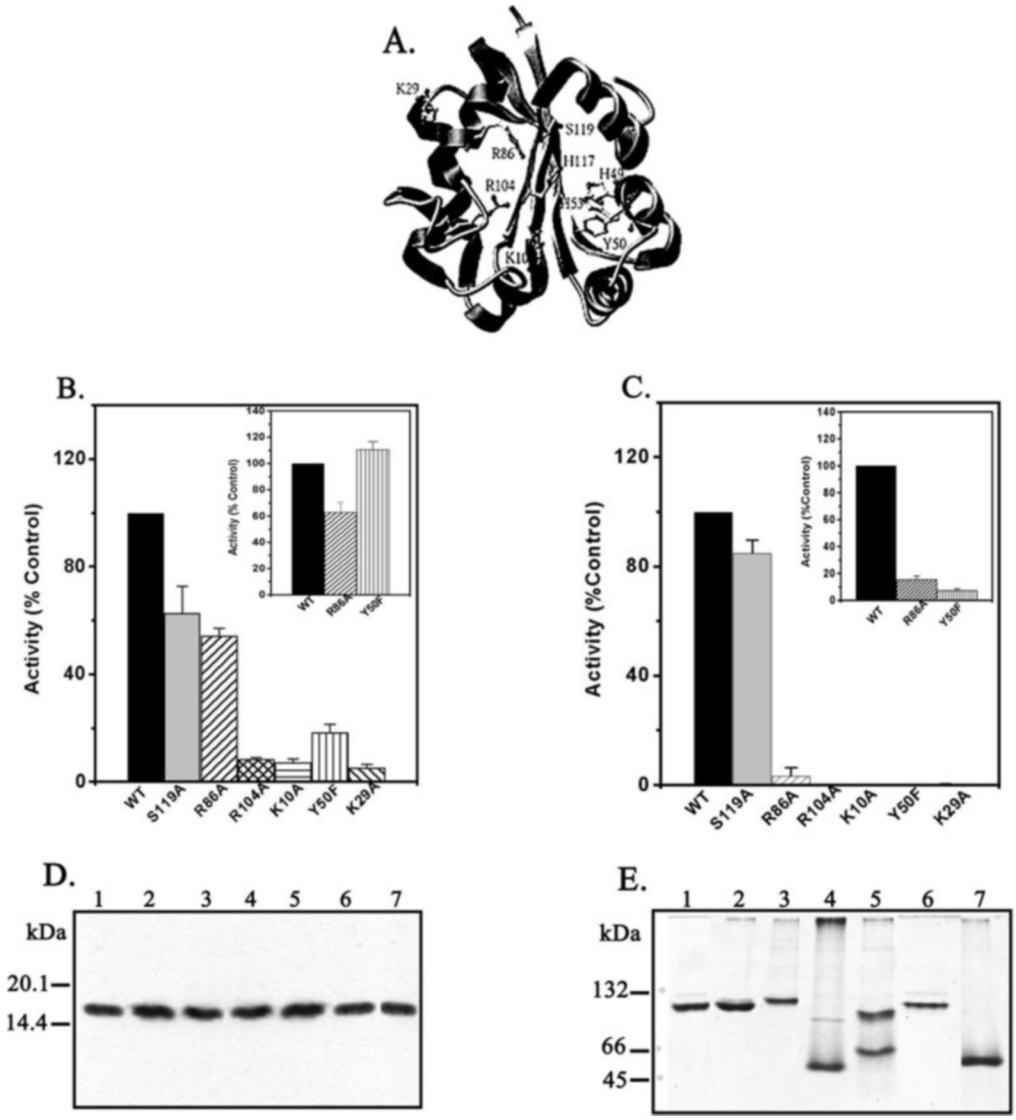

FIG. 6. **Effect of mutations at the active site of the mNdK on its autophosphorylation and phosphotransfer activities.** Mutations at different active site residues of mNdK were generated as described under "Experimental Procedures." Autophosphorylation and phosphotransfer activities of these mutants were compared with those of the wild type enzyme. *A*, position of different amino acid residues at the active site of the mNdK. *B*, autophosphorylation of wild type (*WT*) or different mutants were monitored (250 ng or 2.5 μg of protein per reaction) as described in the text. Signal intensity of different bands obtained with wild type or mutants was measured in a phosphorimaging device. Results (mean ± S.D., n = 3) presented here are band intensities of different mutants as percentage of wild type control using 250 ng of protein per reaction. *Inset*: autophosphorylation of R86A and Y50F mutants (2.5 μg of protein per reaction) as percentage of wild type control. *C*, phosphotransfer activities of different mutants were assayed as described under "Experimental Procedures " using 5, 50, and 250 ng of proteins per reaction. The results (mean ± S.D., n = 3) presented here are the phosphotransfer activities of different mutants expressed as the percentage of wild type control using 5 ng of protein per reaction. *Inset*: phosphotransfer activities of R86A and Y50F mutants compared with the wild type using 250 ng of protein in assays. *D*, Western blot analysis of mutant proteins using anti-mNdK antibody. *Lane 1*, wild type NdK; *lane 2*, S119A; *lane 3*, R86A; *lane 4*, R104A; *lane 5*, K10A; *lane 6*, Y50F; *lane 7*, K29A. *E*, native-PAGE analysis of mutant proteins. Samples (wild type and mutant proteins) were resolved in a 9% native PAGE and stained with Coomassie Brilliant Blue. *Lane 1*, wild type NdK; *lane 2*, S119A; *lane 3*, R86A; *lane 4*, R104A; *lane 5*, K10A; *lane 6*, Y50F; *lane 7*, K29A. Positions of molecular weight standards are indicated.

(46–51). Three histidine residues (positions 49, 53, and 117) were observed at the active site of mNdK (Fig. 6*A* and Ref. 28). Because mNdK is a histidine kinase, we investigated the contributions of these histidine residues in the autophosphorylation and phosphotransfer activities of the protein. Each of the histidine residues was mutated to either alanine (a polar to hydrophobic substitution) or glutamine (a polar to polar substitution). All the mutants, except for H117A/H117Q incorporated γ-^{32}P from ATP as well as the wild type control (Fig. 4*B*). Thus we conclude that His-117 of the mNdK is the residue at the active site of the protein that is essential for autophosphorylation (Fig. 4*B*). On the other hand, except for H49A/H49Q, the phosphotransfer activities of the other mutants (H53A/H53Q and H117A/H117Q) were seriously affected, which was evident from the significant decrease in V_{max} and k_{cat}/K_m values despite an unaltered K_m (Table II). In fact, H117A/H117Q showed so little phosphotransfer activity that the kinetic parameters could not be determined (Table II). Thus our results contrast with the report that mutation of the histidine residues of NdK from *M. tuberculosis* strain H37Rv did not affect phosphotransfer activity (27).

We further examined the contribution of these histidine residues toward the functionality of mNdK through a genetic approach. It has been shown that, in the absence of NdK, pyruvate kinase is involved in maintaining NTP pools in *P. aeruginosa* (5). As a consequence, *ndk*-negative *P. aeruginosa* exhibited slow growth in the presence of a pyruvate kinase inhibitor, Tween 20 (5). We therefore constructed a *ndk*-

disrupted strain, WT^d, and as expected, it exhibited slow growth compared with the wild type *P. aeruginosa* in the presence of Tween 20 (Fig. 5*A*, *left panel*). We further assessed the ability of mNdK and different mutants (H49A/H49Q, H53A/H53Q, and H117A/H117Q) to complement the growth defect of WT^d in the presence of Tween 20. Interestingly, the growth pattern of WT^d harboring the *M. tuberculosis ndk* gene was comparable to that of the wild type *P. aeruginosa* (Fig. 5*A*, both *left* and *right panels*). Among the different mutants, although H49A/H49Q behaved like mNdK (Fig. 5*B*, *left panel*), H117A/H117Q were unable to complement the biological function of the mutant gene (Fig. 5*B*, *right panel*). The results with H53A/H53Q indicated that these mutants were not functionally as efficient as mNdK (Fig. 5*B*, *middle panel*). Thus, the biological activities of all of these mutants correlated well with the phosphotransfer activities (Fig. 5*B* and Table II) and unambiguously established the contributions of both His-53 and His-117 to the cellular functions of mNdK. Furthermore, His-117 is essential for autophosphorylation of mNdK (Fig. 3). The observation that a phosphorylated His-117 in mNdK was unable to carry out subsequent transfer of phosphate to NDPs argues that His-53 plays an important role in regulating this process.

NdK-catalyzed reactions are an excellent example of enzymatic phosphate transfers where P–N and P–O bonds are being formed or broken depending on the steps considered (48). In this regard, the R86A and Y50F mutants of mNdK exhibited interesting behaviors. Both mutants retained a native-like protein conformation, as judged by native PAGE gel analysis (Fig. 6*E*). Although the R86A mutant retained autophosphorylating ability, its phosphotransfer activity was seriously affected (Fig. 6, *B* and *C*). The identical mutation in *D. discoideum* and *D. melanogaster* NdKs exhibited negligible phosphotransfer activities (48, 49). On the other hand, the autophosphorylating ability of the Y50F mutant was restored to the level of the wild type enzyme at high protein concentrations (*inset* of Fig. 6*B*). Because mNdK was predominantly autophosphorylated at the His-117 residue (Fig. 4*B*), our results with the Y50F mutant argued the contribution of Tyr-50 in P–N bond (γ-P of NTP covalently bound to Nδ of His-117) formation is to stabilize the incoming NTP molecule in the transition state. It has already been postulated that the phenyl hydroxyl group of Tyr-50 in NdK interacts with the putative intermediates by lowering the activation barrier (47). In this scenario, the activation energy for autophosphorylation of His-117 in the Y50F mutant would likely be higher than that of the wild type mNdK. Therefore, increasing the amount of mutant protein may compensate for the yield of phosphorylated intermediate in the autophosphorylation reaction (*inset* of Fig. 6*B*). However, this mutant did not show any phosphotransfer activity (Fig. 6*C*), presumably due to destabilization of the network of hydrogen bonds between the phosphohistidine moiety and the phenyl hydroxyl group of the tyrosine residue (47, 48). In fact, the reduced activity resulting from the substitution of tyrosine with phenylalanine could not be overcome by using an excess of protein in the phosphotransfer assays (*inset* of Fig. 6*C*). Thus our results are the first to demonstrate the important contribution of the Tyr-50 residue in the autophosphorylation of mNdK, which may have broad implications in view of the conserved active site residues in different NdKs (46–51).

Identical sequences at the nucleotide level of *ndk* between pathogenic (H37Rv) and nonpathogenic (H37Ra) strains of *M. tuberculosis* presumably indicated similarity in the nature of the proteins. This is not unusual considering the "housekeeping" function of mNdK, such as maintaining cellular NTP pools. However, it is intriguing that purified NdK from a pathogenic mycobacteria (*M. tuberculosis* strain H37Rv) facilitated ATP-dependent P2Z receptor-mediated mouse macrophage cell death (27), whereas that from a nonpathogenic strain (*M. bovis* bacillus Calmette-Guérin) prevented it (19). Therefore, further work is necessary to understand the role of mNdK in apoptotic death of macrophages during infection. Finally, our study examined some structure/activity relationships of mNdK and unequivocally established that several amino acid residues are required either for autophosphorylation or phosphotransfer but not both activities of the protein.

Acknowledgments—We are thankful to Dr. A. Ghosh, Director, Institute of Microbial Technology for providing us with excellent laboratory facilities. We are grateful to Dr. S. Stoney Simons, Jr., Chief, Steroid Hormones Section, Laboratory of Molecular and Cellular Biology, NIDDK, National Institutes of Health, Bethesda, MD for critically reading the manuscript. We acknowledge the receipt of the expression plasmid pSFFLAG-MAC and *P. aeruginosa* type strain (MTCC 1934) as gifts from Dr. Robin Couch, Rice University, Houston, TX and the Microbial Type Culture Collection, Chandigarh, India, respectively. We thank Drs. D. Sarkar, A. Mondal, G. Varshney, P. Guptasarma, and S. Thomas for extending help whenever necessary during the course of this investigation. We are thankful to J. Prasad for providing us with excellent technical assistance.

REFERENCES

1. Lascu, I., and Gonin, P. (2000) *J. Bioenerg. Biomembr.* **32,** 237–246
2. Munoz-Dorado, J., Inouye, M., and Inouye, S. (1990) *J. Biol. Chem.* **265,** 2702–2706
3. Lacombe, M. L., Wallet, V., Troll, H., and Veron, M. (1990) *J. Biol. Chem.* **265,** 10012–10018
4. Hama, H., Almaula, N., Lerner, C. G., Inouye, S., and Inouye, M. (1991) *Gene* (*Amst.*) **105,** 31–36
5. Sundin, G. W., Shankar, S., Chugani, S. A., Chopade, B. A., Kavanaugh-Black, A., and Chakrabarty, A. M. (1996) *Mol. Microbiol.* **20,** 965–979
6. Lacombe, M. L., Milon, L., Munier, A., Mehus, J. G., and Lambeth, D. O. (2000) *J. Bioenerg. Biomembr.* **32,** 247–258
7. Lascu, I., Giartosio, A., Ransac, S., and Erent, M. (2000) *J. Bioenerg. Biomembr.* **32,** 227–236
8. Lu, Q., Park, H., Egger, L. A., and Inouye, M. (1996) *J. Biol. Chem.* **271,** 32886–32893
9. Postel, E. H., Berberich, S. J., Rooney, J. W., and Kaetzel, D. M. (2000) *J. Bioenerg. Biomembr.* **32,** 277–284
10. Postel, E. H., Abramczyk, B. M., Levit, M. N., and Kyin, S. (2000) *Proc. Natl. Acad. Sci. U. S. A.* **97,** 14194–14199
11. Fan, Z., Beresford, P. J., Oh, D. Y., Zhang, D., and Lieberman, J. (2003) *Cell* **112,** 659–672
12. Postel, E. H., and Abramczyk, B. M. (2003) *Proc. Natl. Acad. Sci. U. S. A.* **100,** 13247–13252
13. Biggs, J., Hersperger, E., Steeg, P. S., Liotta, L. A., and Shearn, A. (1990) *Cell* **63,** 933–940
14. Lacombe, M. L., Sastre-Garau, X., Lascu, I., Vonica, A., Wallet, V., Thiery, J. P., and Veron, M. (1991) *Eur. J. Cancer* **27,** 1302–1307
15. Hartsough, M. T., and Steeg, P. S. (2000) *J. Bioenerg. Biomembr.* **32,** 301–308
16. Kimura, N., and Shimada, N. (1988) *J. Biol. Chem.* **263,** 4647–4653
17. Shankar, S., Hershberger, C. D., and Chakrabarty, A. M. (1997) *Mol. Microbiol.* **24,** 477–487
18. Chakrabarty, A. M. (1998) *Mol. Microbiol.* **28,** 875–882
19. Zaborina, O., Li, X., Cheng, G., Kapatral, V., and Chakrabarty, A. M. (1999) *Mol. Microbiol.* **31,** 1333–1343
20. Shankar, S., Kamath, S., and Chakrabarty, A. M. (1996) *J. Bacteriol.* **178,** 1777–1781
21. Gounaris, K., Thomas, S., Najarro, P., and Selkirk, M. E. (2001) *Infect. Immun.* **69,** 3658–3662
22. Punj, V., Zaborina, O., Dhiman, N., Falzari, K., Bagdasarian, M., and Chakrabarty, A. M. (2000) *Infect. Immun.* **68,** 4930–4937
23. Lefevre, P., Braibant, M., de Wit, L., Kalai, M., Roeper, D., Grotzinger, J., Delville, J. P., Peirs, P., Ooms, J., Huygen, K., and Content, J. (1997) *J. Bacteriol.* **179,** 2900–2906
24. Andersen, A. B., and Brennan, P. (1994) in *Tuberculosis: Pathogenesis*, *Protection*, *and Control* (Bloom, B., ed) pp. 307–332, ASM Press, Washington, D. C.
25. Bloom, B. R., and Murray, C. J. (1992) *Science* **257,** 1055–1064
26. Cole, S. T., Brosch, R., Parkhill, J., Garnier, T., Churcher, C., Harris, D., Gordon, S. V., Eiglmeier, K., Gas, S., Barry, C. E., III, Tekaia, F., Badcock, K., Basham, D., Brown, D., Chillingworth, T., Connor, R., Davies, R., Devlin, K., Feltwell, T., Gentles, S., Hamlin, N., Holroyd, S., Hornsby, T., Jagels, K., Krogh, A., McLean, J., Moule, S., Murphy, L., Oliver, K., Osborne, J., Quail, M. A., Rajandream, M. A., Rogers, J., Rutter, S., Seeger, K., Skelton, J., Squares, R., Squares, S., Sulston, J. E., Taylor, K., Whitehead, S., and Barrell, B. G. (1998) *Nature* **393,** 537–544
27. Chopra, P., Singh, A., Koul, A., Ramachandran, S., Drlica, K., Tyagi, A. K., and Singh, Y. (2003) *Eur. J. Biochem.* **270,** 625–634
28. Chen, Y., Morera, S., Mocan, J., Lascu, I., and Janin, J. (2002) *Proteins* **47,** 556–557
29. Chaba, R., Raje, M., and Chakraborti, P. K. (2002) *Eur. J. Biochem.* **269,** 1078–1085
30. Guan, K. L., and Dixon, J. E. (1991) *Anal. Biochem.* **192,** 262–267
31. Couch, R., Seidle, H., and Parry, R. (2002) *BioTechniques* **32,** 1230–1236

32. Ausubel, F. M., Brent, R., Kingston, R. E., Moore, D. D., Seidman, J. G., Smith, J. A., and Struhl, K. (1998) *Current Protocols in Molecular Biology*, John Wiley and Sons, New York
33. Stover, C. K., Pham, X. Q., Erwin, A. L., Mizoguchi, S. D., Warrener, P., Hickey, M. J., Brinkman, F. S., Hufnagle, W. O., Kowalik, D. J., Lagrou, M., Garber, R. L., Goltry, L., Tolentino, E., Westbrock-Wadman, S., Yuan, Y., Brody, L. L., Coulter, S. N., Folger, K. R., Kas, A., Larbig, K., Lim, R., Smith, K., Spencer, D., Wong, G. K., Wu, Z., Paulsen, I. T., Reizer, J., Saier, M. H., Hancock, R. E., Lory, S., and Olson, M. V. (2000) *Nature* **406,** 959–964
34. Oka, A., Sugisaki, H., and Takanami, M. (1981) *J. Mol. Biol.* **147,** 217–226
35. Ho, S. N., Hunt, H. D., Horton, R. M., Pullen, J. K., and Pease, L. R. (1989) *Gene* (*Amst.*) **77,** 51–59
36. Sarin, J., Aggarwal, S., Chaba, R., Varshney, G. C., and Chakraborti, P. K. (2001) *J. Biol. Chem.* **276,** 44590–44597
37. Bradford, M. M. (1976) *Anal. Biochem.* **72,** 248–254
38. Diver, J. M., Bryan, L. E., and Sokol, P.A. (1990) *Anal. Biochem.* **189,** 75–79
39. Sambrook, J., and Russel, D. (2001) *Molecular Cloning: A Laboratory Manual*, Cold Spring Harbor Laboratory Press, Cold Spring Harbor, NY
40. Lascu, I., LeBlay, K., Lacombe, M. L., Presecan, E., and Veron, M. (1993) *Anal. Biochem.* **209,** 6–8
41. Jones, T. A., Zou, J. Y., Cowan, S. W., and Kieldgaard, M. (1991) *Acta Crystallogr. Sect. A* **47,** 110–119
42. Munoz-Dorado, J., Inouye, S., and Inouye, M. (1990) *J. Biol. Chem.* **265,** 2707–2712
43. Anostario, M., Harrison, M., and Geahlen, R. (1990) *Anal. Biochem.* **190,** 60–65
44. Kowluru, A. (2002) *Biochem. Pharmacol.* **63,** 2091–2100
45. Schneider, B., Xu, Y. W., Janin, J., Veron, M., and Deville-Bonne, D. (1998) *J. Biol. Chem.* **273,** 28773–28778
46. Schneider, B., Babolat, M., Xu, Y. W., Janin, J., Veron, M., and Deville-Bonne, D. (2001) *Eur. J. Biochem.* **268,** 1964–1971
47. Tepper, A., Dammann, H., Bominaar, A., and Veron, M. (1994) *J. Biol. Chem.* **269,** 32175–32180
48. Morera, S., Chiadmi, M., LeBras, G., Lascu, I., and Janin, J. (1995) *Biochemistry* **34,** 11062–11070
49. Janin, J., Dumas, C., Morera, S., Xu, Y., Meyer, P., Chiadmi, M., and Cherfils, J. (2000) *J. Bioenerg. Biomembr.* **32,** 215–225
50. Min, K., Song, H. K., Chang, C., Kim, S. Y., Lee, K. J., and Suh, S. W. (2002) *Proteins* **46,** 340–342
51. Postel, E. H., Abramczyk, B. M., Gursky, S. K., and Xu, Y. (2002) *Biochemistry* **41,** 6330–6337